Pulse duration dependent nonlinear propagation of a focused femtosecond laser pulse in fused silica

Quan Sun, Hidenori Asahi, Yoshiaki Nishijima, Naoki Murazawa, Kosei Ueno, and Hiroaki Misawa*

Research Institute for Electronic Science, Hokkaido University, Sapporo 001-0021, Japan

**misawa@es.hokudai.ac.jp*

Abstract: The nonlinear propagation of a single focused femtosecond laser pulse in fused silica has been investigated both experimentally and by numerical simulations. In particular, the filamentation behavior was systematically studied by varying pulse duration. At low pulse energy, the peak plasma density inside the filament first increases to a maximum value with increasing pulse duration and then begins to decrease. At relatively high pulse energy, denser plasma can be induced around the geometrical focus with a certain longer pulse duration, where the peak power is already below the self-focusing critical power and no filament is formed. This pulse duration dependent behavior can be explained by different ionization mechanisms.

OCIS codes: (320.7110) Ultrafast nonlinear optics; (320.7130) Ultrafast processes in condensed matter, including semiconductors; (140.3390) Laser materials processing.

References and links

1. S. L. Chin, S. A. Hosseini, W. Liu, Q. Luo, F. Théberge, N. Akozbek, A. Becker, V. P. Kandidov, O. G. Kosareva, and H. Schroeder, "The propagation of powerful femtosecond laser pulses in optical media: physics, applications, and new challenges," Can. J. Phys. **83**, 863 (2005).
2. A. Couairon and A. Mysyrowicz, "Femtosecond filamentation in transparent media," Phys. Rep. **441**, 47 (2007).
3. J. Kasparian and J. P. Wolf, "Physics and applications of atmospheric nonlinear optics and filamentation," Opt. Express **16**, 466 (2008).
4. A. Brodeur, C. Y. Chien, F. A. Ilkov, S. L. Chin, O. G. Kosareva, and V. P. Kandidov, "Moving focus in the propagation of ultrashort laser pulses in air," Opt. Lett. **22**, 304 (1997).
5. J. Kasparian, M. Rodriguez, G. Mejean, J. Yu, E. Salmon, H. Wille, R. Bourayou, S. Frey, Y.-B. Andre, A. Mysyrowicz, R. Sauerbrey, J.-P. Wolf, and L. Woste, "White-Light Filaments for Atmospheric Analysis," Science **301**, 61 (2003).
6. W. Liu, F. Théberge, E. Arevalo, J.-F. Gravel, A. Becker, and S. L. Chin, "Experiment and simulations on the energy reservoir effect in femtosecond light filaments," Opt. Lett. **30**, 2602 (2005).
7. Y. Ma, X. Lu, T. Xi, Q. Gong, and J. Zhang, "Widening of Long-range femtosecond laser filaments in turbulent air," Opt. Express **16**, 8332 (2008).
8. Y. Fu, H. Xiong, H. Xu, J. Yao, B. Zeng, W. Chu, Y. Cheng, Z. Xu, W. Liu, and S. L. Chin, "Generation of extended filaments of femtosecond pulses in air by use of a single-step phase plate," Opt. Lett. **34**, 3752 (2009).
9. S. Tzortzakis, L. Sudrie, M. Franco, B. Prade, and A. Mysyrowicz, "Self-Guided Propagation of Ultrashort IR Laser Pulses in Fused Silica," Phys. Rev. Lett. **87**, 213902 (2001).
10. W. Liu, S. Petit, A. Becker, N. Akozbek, C. M. Bowden, and S. L. Chin, "Intensity clamping of a femtosecond laser pulse in condensed matter," Opt. Commun. **202**, 189 (2002).
11. L. Sudrie, A. Couairon, M. Franco, B. Lamouroux, B. Prade, S. Tzortzakis, and A. Mysyrowicz, "Femtosecond Laser-Induced Damage and Filamentary Propagation in Fused Silica," Phys. Rev. Lett. **89**, 186601 (2002).
12. N. T. Nguyen, A. Saliminia, W. Liu, S. L. Chin, and R. Vallee, "Optical breakdown versus filamentation in fused silica by use of femtosecond infrared laser pulses," Opt. Lett. **28**, 1591 (2003).

#134830 - $15.00 USD Received 8 Sep 2010; revised 28 Oct 2010; accepted 29 Oct 2010; published 9 Nov 2010

13. Z. Wu, H. Jiang, Q. Sun, H. Yang, and Q. Gong, "Filamentation and temporal reshaping of a femtosecond pulse in fused silica," Phys. Rev. A **68**, 063820 (2003).
14. S. Onda, W. Watanabe, K. Yamada, and K. Itoh, "Study of filamentary damage in synthesized silica induced by chirped femtosecond laser pulses," J. Opt. Soc. Am. B **11**, 2437 (2005).
15. Q. Sun, H. Jiang, Y. Liu, Y. Zhou, H. Yang, and Q. Gong, "Effect of spherical aberration on the propagation of a tightly focused femtosecond laser pulse inside fused silica," J. Opt. A, Pure Appl. Opt. **7**, 655 (2005).
16. A. Couairon, L. Sudrie, M. Franco, B. Prade, and A. Mysyrowicz, "Filamentation and damage in fused silica induced by tightly focused femtosecond laser pulses," Phys. Rev. B **71**, 125435 (2005).
17. E. Gaizauskas, E. Vanagas, V. Jarutis, S. Juodkazis, V. Mizeikis, and H. Misawa, "Discrete damage traces from filamentation of Gauss-Bessel pulses," Opt. Lett. **31**, 80 (2006).
18. V. Mizeikis, S. Juodkazis, T. Balciunas, H. Misawa, S. I. Kudryashov, V. D. Zvorykin, and A. A. Ionin, "Optical and ultrasonic signatures of femtosecond pulse filamentation in fused silica," J. Appl. Phys. **105**, 123106 (2009).
19. W. Liu, O. Kosareva, I. S. Golubtsov, A. Iwasaki, A. Becker, V. P. Kandidov, and S. L. Chin, "Femtosecond laser pulse filamentation versus optical breakdown in H2O," Appl. Phys. B **76**, 215 (2003).
20. A. Dubietis, A. Couairon, E. kucinskas, G. Tamosauskas, E. Gaizauskas, D. Faccio, and P. D. Trapani, "Measurement and calculation of nonlinear absorption associated with femtosecond filaments in water," Appl. Phys. B **84**, 439 (2006).
21. D. Faccio, M. A. Porras, A. Dubietis, G. Tamosauskas, E. Kucinskas, A. Couairon, and P. D. Trapani, "Angular and chromatic dispersion in Kerr-driven conical emission," Opt. Commun. **265**, 672 (2006).
22. S. Minardi, A. Gopal, M. Tatarakis, A. Couairon, G. Tamosauskas, R. Piskarskas, A. Dubietis, and P. D. Trapani, "Time-resolved refractive index and absorption mapping of light-plasma filaments in water," Opt. Lett. **33**, 86 (2008).
23. J. Yu, H. Jiang, J. Wen, H. Yang, and Q. Gong, "Mechanism of depolarization of white light generated by femtosecond laser pulse in water," Opt. Express **18**, 12581 (2010).
24. A. Saliminia, R. Vallee, and S. L. Chin, "Waveguide writing in silica glass with femtosecond pulses from an optical parametric amplifier at 1.5 um," Opt. Commun. **256**, 422 (2005).
25. H. Guo, H. Jiang, Y. Fang, C. Peng, H. Yang, Y. Li, and Q. Gong, "The pulse duration dependence of femtosecond laser induced refractive index modulation in fused silica," J. Opt. A, Pure Appl. Opt. **6**, 787 (2004).
26. Q. Sun, A. Saliminia, F. Théberge, R. Vallee, and S. L. Chin, "Microchannel fabrication in silica glass by femtosecond laser pulses with different central wavelengths," J. Micromech. Microeng. **18**, 035039 (2008).
27. J. F. Herbstman and A. J. Hunt, "High-aspect ratio nanochannel formation by single femtosecond laser pulses," Opt. Express **18**, 16840 (2010).
28. K. Yamada, W. Watanabe, Y. Li, K. Itoh, and J. Nishii, "Multilevel phase-type diffractive lenses in silica glass induced by filamentation of femtosecond laser pulses," Opt. Lett. **29**, 1846 (2004).
29. J. H. Marburger, "Self-focusing: theory," Prog. Quantum Electron. **4**, 35 (1975).
30. W. Liu and S. Chin, "Direct measurement of the critical power of femtosecond Ti:sapphire laser pulse in air," Opt. Express **13**, 5750 (2005).
31. L. V. Keldysh, "Ionization in the field of a strong electromagentic wave," Sov. Phys. JETP **20**, 1307 (1965).
32. Q. Sun, H. Jiang, Y. Liu, Z. Wu, H. Yang, and Q. Gong, "Measurement of the collision time of dense electronic plasma induced by a femtosecond laser in fused silica," Opt. Lett. **30**, 320 (2005).
33. M. Mlejnek, E. M. Wright, and J. V. Moloney, "Dynamic spatial replenishment of femtosecond pulses propagating in air," Opt. Lett. **23**, 382 (1998).
34. Y. Liu, H. Jiang, Q. Sun, Z. Wu, H. Yang, and Q. Gong, "Different tendencies of breakdown threshold on pulse duration in the subpicosecond regime in fused silica," J. Opt. A, Pure Appl. Opt. **7**, 198 (2005).

1. Introduction

Femtosecond laser interactions with optical media have been intensively investigated for several decades, especially after the invention of chirped pulse amplification (CPA), which prompted the wide spread use of femtosecond lasers. Because high intensities can be easily obtained by femtosecond lasers, many nonlinear optical processes arise. Among these processes, filamentation has attracted much attention [1–3]. When the input power of the femtosecond laser pulses is above a critical power P_{cr} for self-focusing (SF), filamentation can be induced in air [4–8], solids [9–18], and liquids [19–23]. Because the nonlinear refraction index of transparent solids, such as fused silica, is about 3 orders of magnitude larger than that of air, the critical power for SF in solids is in the megawatt range. Therefore, it is easier to obtain filamentation in solids with low pulse energy (typically on the order of μJ) in laboratories. Filamentation in solids has also triggered many applications, including fabrications of waveguides [24], gratings [25], microchannels [26], nanochannels [27], Fresnel plates [28] and other photonic components.

#134830 - $15.00 USD Received 8 Sep 2010; revised 28 Oct 2010; accepted 29 Oct 2010; published 9 Nov 2010

A better understanding of the filamentation in solids is crucial not only for enrichment of the knowledge for nonlinear optics, but also for further guiding the development of applications. Recently, the dependence of filamentation in fused silica on the focusing condition [12, 13] and pulse energy [13] have been reported. However, the research on the effect of the pulse duration on the filamentation in transparent solids by a single pulse is still lacking, though the pulse duration on filamentation assisted microfabrication [25] by a femtosecond laser has been investigated.

In this paper, we report on the investigation of the filamentation of near infrared (NIR) femtosecond laser pulses in fused silica with varied pulse durations. For a given pulse energy, an increase of the pulse duration results in a decrease of the peak power. As expected, the filament length decreases with an increase in the pulse duration because of the decrease of the peak power. However, we find that, at low pulse energy the peak plasma density inside the filament increases to a maximum and then decreases as the pulse duration is increased. The numerical simulations give similar results. We explain the results in terms of different degrees of contribution from multiphoton ionization (MPI) and avalanche under different pulse durations. We also investigate the pulse duration dependent behavior at higher pulse energy, where avalanche can lead to dense electron plasma at the long pulse durations, in which the filamentation cannot be triggered. In addition, our findings provide useful information for the microfabrication of photonic devices or components in fused silica.

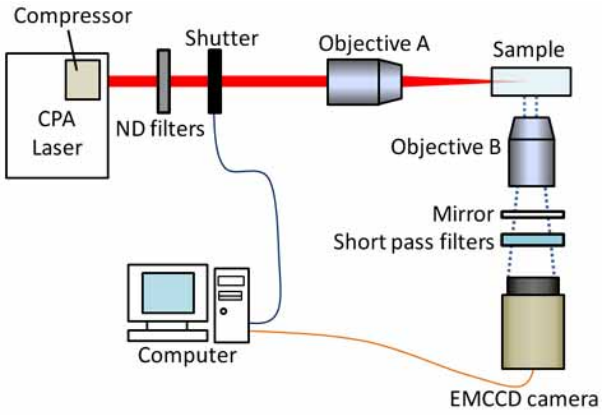

Fig. 1. Experimental setup.

2. Experimental

The schematic for the experimental setup is shown in Fig. 1. A Ti: sapphire CPA femtosecond laser system (Spitfire, Spectra Physics) was used in the experiment. The central wavelength of the output laser pulses is 800 nm, and the repetition rate is 1 kHz but can be tuned between 1 Hz and 1 kHz. The laser beam passed through two neutral density (ND) filters, and was then focused into bulk fused silica by an objective lens (Olympus, 4×) with a numerical aperture (NA) of 0.13. The bulk sample with all surfaces well polished had dimensions of $5\ mm \times 10\ mm \times 20\ mm$) and was mounted on a three dimensional stage. The laser interaction region, which is the filament zone, was imaged onto an EMCCD camera(C9100-14, Hamamatsu) by another long working distance objective lens B (Mitutoyo, 20×, NA = 0.40). To enable single shot irradiation, the laser repetition rate was set at 100 Hz and an electronic shutter synchronous with the EMCCD was employed to select a single pulse (the opening time of

#134830 - $15.00 USD Received 8 Sep 2010; revised 28 Oct 2010; accepted 29 Oct 2010; published 9 Nov 2010

the shutter was set at 8 ms). Before the EMCCD, one 800 nm mirror (0°) and two short pass filters (transmission: 350 nm-700 nm) were used to block the scattered 800 nm laser light, and thus the plasma luminescence in the visible region from the laser interaction region was imaged by EMCCD and processed by a computer. The resolution of imaging system is 0.7 μm. The distribution of the electron plasma density could be qualitatively characterized by the intensity of the plasma luminescence. After every laser shot, the sample was translated by 50 μm in vertical direction. In our experiments, the pulse duration was tuned by changing the separation distance of the grating used in the compressor of the Spitfire system and was measured by a single shot autocorrelator (SSA, Positive Light), allowing the investigation of the pulse duration dependent filamentation to be achieved.

3. Results and discussion

The laser pulse was focused at a depth of 600 μm inside the sample. For a fixed pulse energy of 2.7 μJ, the plasma luminescence with different pulse durations was recorded by the EMCCD, and the images are shown in Fig. 2. The dashed line indicates the position of the geometrical focus. The longest plasma channel (filament) is formed by the 80 fs pulse but has a slight negative chirp, as shown in Fig. 2(a). At the measured shortest pulse duration [45fs, Fig. 2(b)], the filament length decreases. With the introduction of a positive chirp, the pulse duration increases and the filament length further decreases as shown in Fig. 2(b) to 2(d). When the pulse duration reaches 1200 fs and ever longer, the filamentation is replaced by a breakdown located at the geometrical focus [Fig. 2(e) and 2(f)].

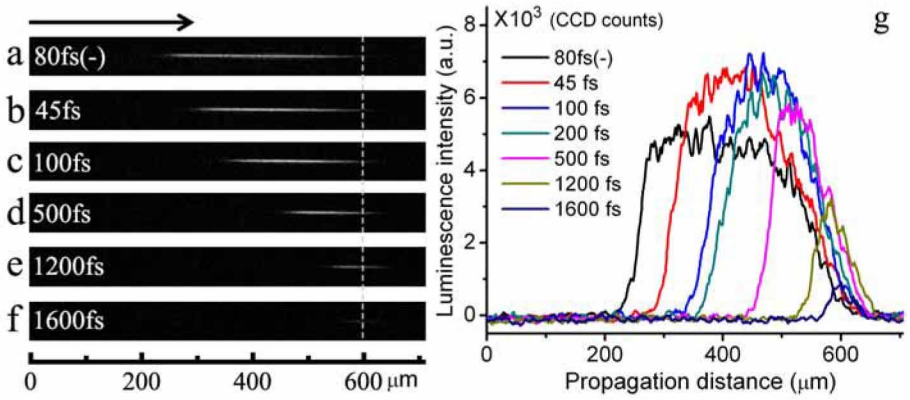

Fig. 2. EMCCD images (a)–(f) and the plot of on-axis relative intensities (g) of plasma luminescence induced by a single focused ultrashort pulse with different pulse durations. The energy of the pulse is fixed at 2.7 μJ. The arrow indicates the laser propagation direction, and the zero position is located at the incident surface of the sample.

The above results can be understood with the slice by slice model for filamentation [4]. In this model, the onset of the filamentation in a homogeneous Kerr medium for parallel Gaussian beams is determined by the SF distance, Z_f, which can be given by the Marburger formula [29, 30]:

$$Z_f = \frac{0.367ka^2}{\{[(P/P_{cr})^{1/2} - 0.852]^2 - 0.0219\}^{1/2}}, \quad (1)$$

where ka^2 indicates the diffraction length, k is the wavenumber and a is the radius at the $1/e$ level of the beam profile. P_{cr} is estimated to be 2.7 MW for fused silica. In the case of external

#134830 - $15.00 USD Received 8 Sep 2010; revised 28 Oct 2010; accepted 29 Oct 2010; published 9 Nov 2010

focusing, the onset position (Z) of the filamentation should be determined by both Z_f and the external focal length f as,

$$Z = \frac{Z_f f}{Z_f + f}. \tag{2}$$

In the current experimental situation, f is the distance between the geometrical focus and the front surface of the glass sample, and Z is the distance of the starting point from the front surface. It is noted that the filaments observed in our experiments are almost concluded at the geometrical focus, and thus the filament length can be expressed as $L = f - Z = f^2/(Z_f + f)$. For fixed f, L is dependent on the peak power (P) of the pulse. At a fixed pulse energy, a longer pulse duration, lower peak power, and a shorter filament length is expected as shown in Fig. 2. We have to note that, the longest filament occurs in Fig. 2(a), where the pulse duration is negatively chirped to 80 fs. This phenomenon is due to the measurement of the pulse duration at the output of the laser system, because it is very difficult to measure the pulse duration after the focusing objective lens and impossible to measure the accurate pulse duration at the geometrical focus inside the sample. Considering the group velocity dispersion (GVD) induced during the propagation in ND filters, objective lens, and the glass sample before reaching the geometrical focus, we estimate that the nominal transfer limited pulse (45 fs) in Fig. 2(b) is lengthened to 60-80 fs. Thus, the negative chirp introduced in Fig. 2(a) is mostly to compensate the positive chirp induced by this GVD effect, and the real pulse duration at the geometrical focus should be close to or slightly larger than the transfer limited pulse duration (45 fs). Accordingly, the real pulse durations at the geometrical focus should be slightly larger than those listed in Fig. 2(c)–2(f). In addition, when the pulse duration is large enough that the pulse peak power is lower than the critical power, filamentation cannot be launched, and the plasma is only located around the geometrical focus, as shown in Fig. 2(e)and 2(f), where the peak power is only 0.833 P_{cr} and 0.625 P_{cr}, respectively.

We note that the most attractive feature in these results is that the peak plasma density is dependent on the pulse duration. With an increase in the pulse duration the peak plasma density first increases and then decreases as shown in Fig. 2(g), which is the plot of the on-axis profile of the plasma luminescence at different pulse duration. To understand this behavior, we must discuss the mechanisms of the formation of the electron plasma. For long pulses (typically nanosecond pulses), free electrons are usually generated by avalanche ionization, which involves free carrier absorption followed by impact ionization, while for short pulses (especially sub-100 fs pulses), photonionization including MPI and/or tunneling ionization plays more important role in the excitation of electrons. The transition from MPI to tunneling ionization can be characterized by the Keldysh adiabaticity parameter for parameter [31],

$$\gamma = \frac{\omega_0}{e}\sqrt{\frac{m_e c n \varepsilon_0 E_g}{I}}, \tag{3}$$

where m_e and e are the effective mass and charge of the electron, respectively, E_g is the band gap energy of the material, c is the speed of light in vacuum, n is the refractive index of the material, ε_0 is the electric permittivity, and I is the intensity of the laser field at frequency ω_0. When γ is much larger than unity, MPI dominates the excitation process. In our case, γ is calculated to be 1.5 if we consider the intensity inside the filament zone as a clamped intensity of $5 \times 10^{13}\ W/cm^2$, as reported for filamentation in air [1]. Actually, the clamped intensity in fused silica should be lower than that in air [26], and thus γ is even larger than 1.5. However, γ is still not large enough to eliminate the contribution from tunneling ionization. It is fairer to say the photonionization here is generally optical field ionization characterized by an adiabaticity parameter that is neither in the validity range of MPI, nor in that of tunnel

#134830 - $15.00 USD Received 8 Sep 2010; revised 28 Oct 2010; accepted 29 Oct 2010; published 9 Nov 2010

ionization. For the convenience in discussion, we only consider MPI here. The rate of MPI is dependent on the intensity. Because of the intensity clamping effect [1,2,10], the rate of MPI is almost constant with varying the pulse durations when the laser peak power exceeds the critical power. The avalanche ionization is dependent on both intensity and the pulse duration because it requires enough time for free carrier absorption through electron-phonon scattering. The time for absorption of one photon is characterized by the electron collision time τ, which has been measured as about 2 fs for fused silica [32]. Thus, to obtain sufficient energy to exceed the band gap energy, the necessary time is on the order of 10 fs. When the pulse duration is extremely short ($<$ 100 fs), the contribution from avalanche may be insignificant because only few cycles of avalanche can be involved, while with an increase in the pulse duration, its contribution should increase at constant intensity, which can be guaranteed because of intensity clamping in the strong filamentation regime. Thus, the initial increase in plasma density with increased pulse duration shown in Fig. 2(g) can be contributed to increased role of avalanche effect. When the pulse duration is further increased, the SF effect becomes weaker. For example, in Fig. 2(d), the pulse duration is 500 fs, and the corresponding peak power of the pulse is only $2P_{cr}$; thus, only a very short filament can form. In this case, the high clamped intensity cannot be maintained. As a result, the rate of both MPI and avalanche ionization starts to decrease, which leads to the decrease of the plasma density.

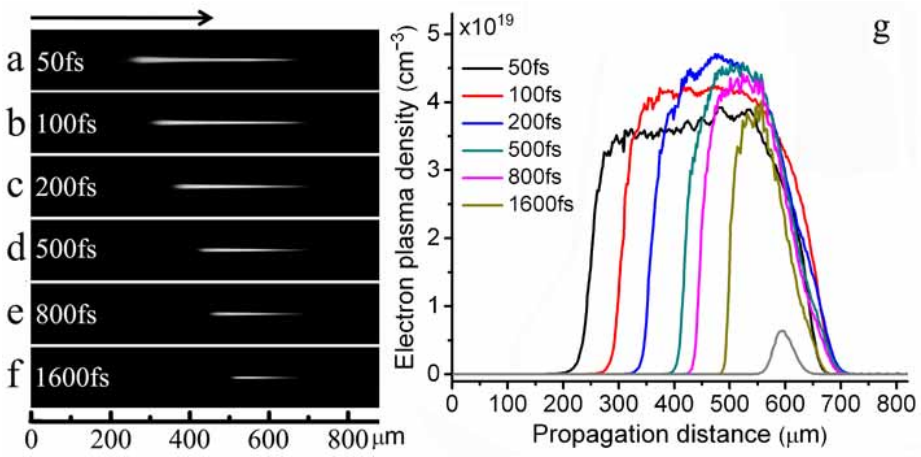

Fig. 3. Numerical results of pulse durations dependent 3D (a)–(f) and on-axis distribution (g) of electron plasma density. The grey curve in (g) is the recalculated result for the case of 1600 fs using 8 fs as τ value, while τ is set as 2 fs for other curves. The pulse energy and the focusing condition are the same as those in Fig. 2. The arrow indicates the laser propagation direction, and the zero position is located at the incident surface of the sample.

To numerically simulate the nonlinear propagation of a single fs laser pulse in fused silica, we adopted a physical model that was developed for intense pulse propagation in various optical media [13, 33, 34]. This model includes two equations:

$$(i2k\frac{\partial}{\partial z}+\nabla_{\perp}^2)E = kk''\frac{\partial^2 E}{\partial \xi^2} - ik\sigma(1+i\omega\tau)\rho E - iK\beta^K|E|^{2K-2}E - 2kk_0n_2|E|^2E, \quad (4)$$

$$\frac{\partial \rho}{\partial \xi} = \frac{1}{n^2}\frac{\sigma}{E_g}\rho|E|^2 + \frac{\beta^{(K)}|E|^{2K}}{K\hbar\omega} - \frac{\rho}{\tau_r}. \quad (5)$$

The details of these two equations can be found in [13, 34]. The parameters k''(GVD coefficient), σ (cross section for inverse bremsstrahlung), τ(electron collision time), n_2(nonlinear

#134830 - $15.00 USD Received 8 Sep 2010; revised 28 Oct 2010; accepted 29 Oct 2010; published 9 Nov 2010

refractive index of fused silica), $\beta^{(K)}$(K-photon absorption coefficient) and τ_r(lifetime of the electron plasma) are taken from the literatures [13, 32, 34]. It is noteworthy that the choice of $\beta^{(K)}$ is an experienced value, which includes the contribution from tunneling ionization [11,13]. Other parameters are adopted from our experimental condition. By solving Eqs. (4) and (5) numerically, Fig. 3 presents the pulse duration dependent 3D electron plasma distribution (ρ) and the profile of the on-axis electron density for an input pulse energy of 2.7 μJ under the same focusing conditions as those in Fig. 2. At the shortest pulse duration, the numerical results produce the longest filament with almost the same length as the experimental result. With increase of the pulse duration, the filament also occurs later. In particular, these numerical results agree well with the experimental results (Fig. 2) regarding the effects of the pulse duration on the on-axis plasma distribution. We also note that, in the simulation results, the plasma density at the longer pulse duration of 1600 fs is still high, whereas in the experimental results, the plasma density decreases more rapidly. This might be due to some simulation parameters being only valid for the filamentation regime. For example, when the pulse duration is too long, such that filamentation is not initiated, only weak plasma can be formed, as experimentally observed in Fig. 2(f). In this case, the electron collision time (τ), which affects the rate of avalanche ionization, should increase. In our simulations, τ is chosen as 2 fs, which is the measured value in the filamentation regime [32]. With this value, the calculated plasma density agrees well with those previously reported [32]. For the case of 1600 fs we also attempted to use different τ values between 2 fs and 23.3 fs, which was used in literatures [11]. Finally, we found the choice of 8 fs, which was close to that (10 fs) used in another literature [16], fitted better with the experimental results, that is, the peak plasma density dropped by one order than that in filamentation regimes. This additional simulation result is plotted as grey curve in Fig. 3(g).

For the case of 1600 fs, we attempted to choose 23.3 fs, which was used by some groups [11], as τ for simulation, and we found that the peak plasma density dropped by a factor of 5 (data not shown). Therefore, if we choose different τ parameters for filamentation region (here, pulse duration should be shorter than 1000 fs) and the longer pulse duration region, the simulations will better fit the experimental results.

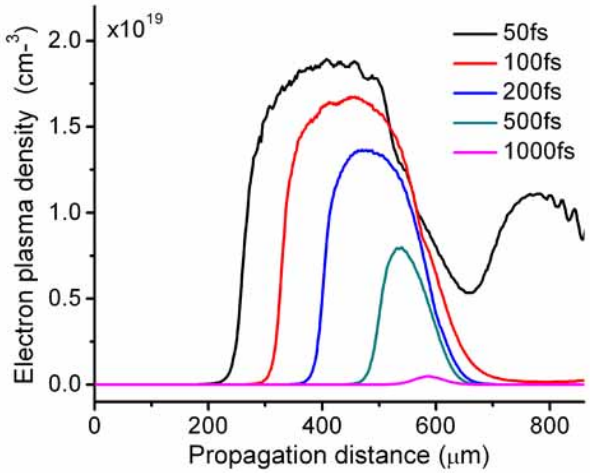

Fig. 4. Numerical results of the pulse duration dependent on-axis distribution of electron plasma density when the avalanche ionization is neglected. The pulse energy and the focusing condition are the same as those in Fig. 2.

In the above simulations, the ionization includes both MPI and avalanche. To confirm the

#134830 - $15.00 USD Received 8 Sep 2010; revised 28 Oct 2010; accepted 29 Oct 2010; published 9 Nov 2010

avalanche contribution, we redid the simulations while omitting the first term on the right-hand side of Eq. (5), which represents the avalanche ionization. The other terms and parameters were the same as those in Fig. 3(g). The results are given in Fig. 4, which clearly shows that the electron plasma density monotonously decreases with increasing pulse duration and decreases much faster at long pulse durations. These results are obviously not consistent with the experimental observation. Therefore, we can conclude that avalanche plays an important role in the nonlinear propagation of femtosecond laser pulses in fused silica and the contribution from avalanche becomes more notable with increasing pulse duration. And, the different role of avalanche is thought to account for the dependence of the electron plasma density on the pulse duration as discussed above. It is worth noting that the avalanche was often neglected or underestimated in previous studies for transparent solids under femtosecond laser irradiation. Actually, the avalanche can almost be neglected for femtosecond laser interaction with air because the collision time for air is much longer (about 350 fs or even longer) [33].

We further investigated the pulse duration dependent nonlinear propagation at relatively high pulse energy. Figure 5 shows the experimental results with a pulse energy of 3.0 μJ. Although the pulse energy is only slightly higher than that used in Fig. 2, the tendency is changed. From (a) to (b), the plasma density still increases. However, further increasing the pulse duration to 1200 fs (b)–(e), the plasma density is almost clamped, and at 1600 fs (f) it suddenly rises, and drops very fast at 2000 fs (g). The clamped peak plasma density from (b) to (e) is mostly due to the intensity clamping in the stronger filamentation regime. At the pulse duration of 1600 fs, the peak power is already below P_{cr}, but high intensity can still be reached at the geometrical focus by external focusing alone, inducing serious avalanche that leads to an increase in plasma density. When the pulse duration increases further, the intensity drops and the avalanche rate also decreases rapidly. Because the tunable range of the pulse duration is wider, as discussed earlier, it is very difficult to determine some parameters. In this case, the numerical investigation was not performed.

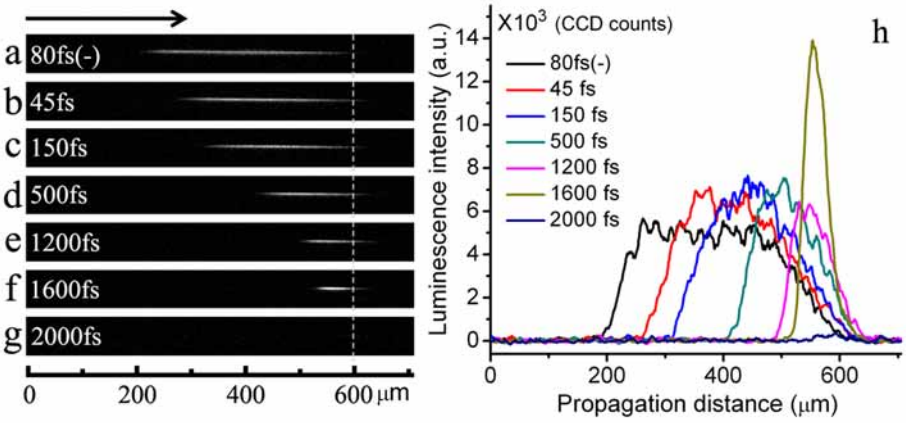

Fig. 5. EMCCD images (a-g) and the plot of the on-axis relative intensities (h) of plasma luminescence induced by a single focused ultrashort pulse with different pulse durations. The energy of the pulse is fixed at 3.0 μJ. The arrow indicates the laser propagation direction, and the zero position is located at the incident surface of the sample.

Our results provide important information for understanding the mechanisms of the nonlinear propagation of femtosecond lasers in transparent materials. From the point of view in the application of femtosecond lasers for material processing and/or microfabrication, the pulse duration is an important parameter. For example, in the case of the fs laser direct writing of waveguides

#134830 - $15.00 USD Received 8 Sep 2010; revised 28 Oct 2010; accepted 29 Oct 2010; published 9 Nov 2010

or gratings using filamentation, short pulse duration might be necessary to obtain smooth modulation of the refractive index. For material ablation or microchannel fabrication, certain long pulse durations may be favorable for achieving high efficiency benefited from avalanche.

4. Conclusions

In summary, we have demonstrated that the nonlinear propagation of a single focused femtosecond laser pulse is dependent on the pulse duration at fixed incident energies. In particular, we both experimentally and numerically investigated the distribution of the electron plasma induced by the laser pulse with different pulse duration at a relative low pulse energy. We found that the peak electron plasma density first increases with the increasing pulse duration and then drops because of the different role of the avalanche in the formation of electron plasma at different pulse durations. At higher pulse energies, much denser electron plasma can be formed with longer pulse durations (when no filamentation occurs) than that in the filamentation regime. The results suggest that varying the pulse duration is an important parameter to consider for fabrication of different devices or components, such as waveguides, gratings, and microchannels in glass, by femtosecond laser pulses.

Acknowledgements

Partial financial support via a Grant-in-Aid from the Ministry of Education, Science, Sports, and Culture of Japan (no. 19049001 for Scientific Research on the Priority Area “Strong Photon-Molecule Coupling Fields for Chemical Reactions” (no. 470) and a Grant-in-Aid from Hokkaido Innovation through Nanotechnology Support (HINTS) are gratefully acknowledged. Q.S. acknowledges the support of the Global COE Program (project no. B01: Catalysis as the Basis from Innovation in Materials Science) from MEXT, Japan.

#134830 - $15.00 USD Received 8 Sep 2010; revised 28 Oct 2010; accepted 29 Oct 2010; published 9 Nov 2010